

CHAPTER 1: INTRODUCTION TO D⁸-D⁸ SYSTEMS

1.1 Background and history

Coordination compounds based on metals with a d⁸ electron configuration have been of interest to chemists for nearly two hundred years. In 1830, Heinrich Magnus first reported the discovery of a green salt prepared from aqueous solutions of [Pt(NH₃)₄]²⁺ and [PtCl₄]²⁻; in 1957, it was discovered that Magnus' salt, rather than being a single molecule like Peyrone chloride (*cis*-PtCl₂(NH₃)₂), was in fact a polymer consisting of alternating [PtCl₄]²⁻ anions and [Pt(NH₃)₄]²⁺ cations.¹ This "polymer" could also be described as a series of d⁸ square planar metal atoms interacting with each other along the coordination axis.

In the 1960s and 70s, the study of d⁸ coordination chemistry was undertaken in earnest by groups such as Gray, Mann, Miskowski, Connick, and others. Researchers began to find that d⁸ compounds, and particularly binuclear d⁸-d⁸ compounds, have access to a range of electronically excited states. This corresponds to a wealth of unique luminescence properties. Although thermal reactivity has always been one of the fundamental tenets of chemistry, the reactivity and applications of electronically excited states has greatly increased in importance and impact since the inception of the field in the mid-1900s.

1.2 Photochemistry of binuclear d⁸-d⁸ metal complexes

D⁸ metal complexes commonly adopt a square-planar geometry with four coordinating ligands.² In a face-to-face dimeric structure of this type, transition metals such as Rh, Ir, and Pt exhibit a

significant amount of metal-metal bonding character in their electronically excited states. This contributes to a rich photochemistry.

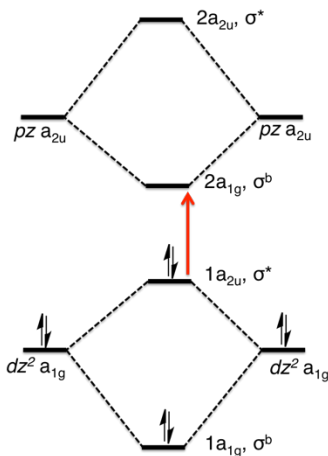


Figure 1: MO diagram of the HOMO to LUMO transition in d^8-d^8 complexes.³

The intense photochemical activity of face-to-face D_{4h} d^8-d^8 complexes is readily explained by a simplified molecular orbital (MO) diagram, as shown in Figure 1. Extensive spectroscopic and theoretical studies have demonstrated that the highest occupied molecular orbital (HOMO) is a $d\sigma^*$ (with respect to M-M bonding) orbital of a_{2u} symmetry and d_{z^2} parentage; specifically, it is a molecular orbital that results from the overlap

of the two metal d_{z^2} (a_{1g}) atomic orbitals. The lowest energy transition is to an orbital of a_{1g} symmetry and p_z parentage. As

this excitation is from an orbital of σ -antibonding character to one of σ -bonding character, the promotion results in the formation of a full metal-metal bond in the excited state as well as the formation of a "hole" at an open coordination site on a metal atom (Figure 2).⁴ The ${}^3(d\sigma^*p\sigma)$ excited state is capable of performing a variety of reactions that would be thermodynamically disfavored for the ground state, including atom abstraction and intermolecular electron transfer.

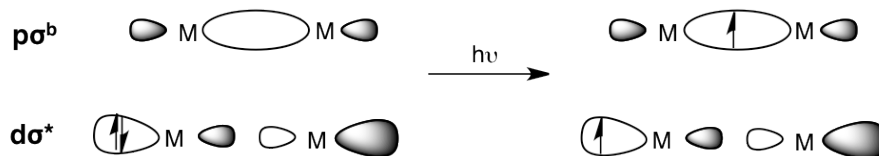


Figure 2: Electron localization on metal MOs.⁴

The study of d^8 - d^8 dimeric compounds has long been a theme in the Gray group. In 1976, researchers in the Gray group first synthesized a dimeric Rh^I complex ligated by four 1,3-diisocyanopropane (“bridge”) moieties. This compound, when irradiated at 546 nm in an aqueous solution of HCl, was found to produce hydrogen gas with concomitant oxidation of the complex to form $[Rh_2(\text{bridge})_4Cl_2]^{2+}$. In 1990, Fox and coworkers studied the kinetics of photoinduced electron transfer d^8 - d^8 Ir_2 phosphonite complexes and demonstrated the existence of an inverted free-energy dependence of electron transfer kinetics at high driving forces. This was one of the first examples of a Marcus “inverted region” in chemical kinetics.⁵

1.3 Remarkable properties of pyrophosphito-bridged diplatinum(II) compounds

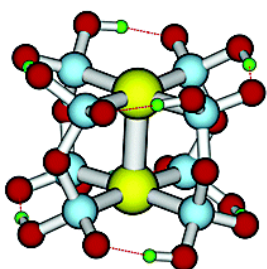


Figure 3: Structure of $Pt(\text{pop})^{4-6}$

One compound that has garnered particular attention is tetrakis(μ -pyrophosphito) diplatinum(II)⁴⁻, also known as ⁴⁻ due to its bridging P-O-P moieties. The compound consists of two d^8 square planar ML_4 fragments supported by pyrophosphito bridges. The two halves are eclipsed, giving rise to a lantern-like complex with D_{4h} symmetry (Figure 3). In the ground state, the Pt-Pt distance is 2.93 Å; while generally this distance is too long to be considered a bond and the molecular orbital (MO) diagram indicates a formal bond order of zero, resonance Raman studies as well as recent theoretical work show that there is indeed some degree of bonding in the ground state due to favorable mixing of the $(n)d_{z^2}$ and $(n+1)p_z$ orbitals.^{8,9}

1.3.1 Photophysical properties

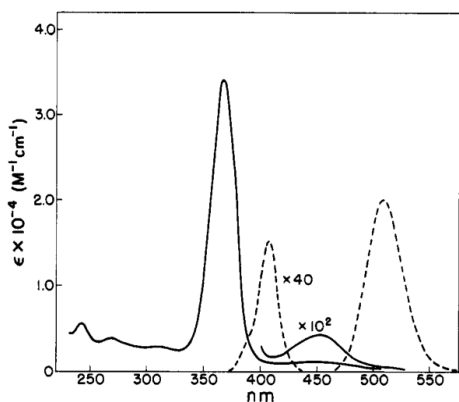


Figure 4: Absorption (solid) and emission (dashed) spectra of the potassium salt of Pt(pop)⁴⁺ in water.⁷

The absorption spectrum of the tetra-*n*-butylammonium salt of Pt(pop)⁴⁺ in MeCN shows an intense electronic absorption band at 372 nm ($\epsilon = 33400 \text{ M}^{-1} \text{ cm}^{-1}$) which is assigned to the $^1A_{1g} \rightarrow ^1A_{2u}$ transition ($d\sigma^* \rightarrow p\sigma$). A much weaker absorption at 454 nm ($\epsilon = 155 \text{ M}^{-1} \text{ cm}^{-1}$) is assigned to the spin-forbidden triplet transition, $^1A_{1g} \rightarrow ^3A_{2u}$.¹⁰

Fluorescence from the $^1(d\sigma^*p\sigma)$ state decays on the picosecond timescale and is quite dependent on

temperature and solvent, while remarkably long-lived phosphorescence (on the order of 10 μs with a quantum yield of 50%) is observed from the $^3(d\sigma^*p\sigma)$ state in a variety of solvents (Figure 4).¹⁰⁻¹²

The lowest energy transition for Pt(pop)⁴⁺, as in other d^8 - d^8 complexes, promotes an electron from a Pt-Pt antibonding $(n)d\sigma^*$ orbital to an $(n+1)p\sigma$ orbital, leading to an increase in the formal bond order and a contraction of the Pt-Pt distance by $\approx 0.24 \text{ \AA}$.¹³ In addition to X-ray studies, the presence of a Pt-Pt bond upon excitation has been investigated by a Franck-Condon analysis of the vibronic progression measured by resonance Raman in the $d\sigma^* \rightarrow p\sigma$ absorption bands in single crystals at low temperatures.⁸

1.3.2 Electron transfer

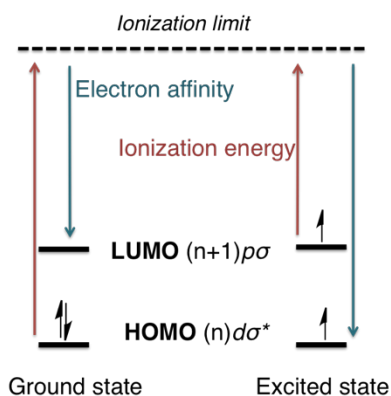


Figure 5: Graphical representation of the enhanced oxidizing (blue) and reducing power (red) of a d⁸-d⁸ compound's excited state.¹¹

Photoexcitation (i.e. promotion of an electron from the HOMO to the LUMO) of Pt(pop)⁴⁺ generates a species that is both a more powerful oxidant *and* reductant than the ground state species. The reducing power of a species (or, its ability to be oxidized and lose an electron) is defined as the energy required to remove its highest-energy

electron (i.e. the ionization energy). The excited state of Pt(pop)⁴⁺ is a better reductant than the ground state because its highest energy electron is in the (n+1)pσ

orbital rather than the (n)dσ* orbital, making that electron easier to remove by an amount of energy equal to the spectroscopic transition.

By a parallel argument, the excited state of Pt(pop)⁴⁺ is a stronger oxidant than the ground state because the oxidizing power of a species is defined by its electron affinity. Since the excited state of Pt(pop)⁴⁺ has a "hole" at the (n)dσ* level, transferring an electron there is more favored than transferring an electron into the LUMO of the ground state, which is the higher energy (n+1)pσ level. These arguments are illustrated in Figure 5.

These general properties of Pt(pop)⁴⁺ combined with the microsecond lifetime of the triplet excited state combine to form a compound that reacts readily with many substrates, including hydrocarbons, alkyl halides, and alcohols.¹⁴ Mechanisms of these reactions may be described as inner-sphere electron transfer processes or as photochemical oxidative addition involving transfer of hydrogen or halogen atoms.

1.3.3 Known reactions of $\text{Pt}(\text{pop})^4$

$\text{Pt}(\text{pop})^4$ undergoes thermal two-electron, two-center oxidative additions of halogens or alkyl halides to produce axially substituted diplatinum(III) complexes Pt_2X_2 or Pt_2RX . These diamagnetic complexes possess an intermetallic bond joining the Pt^{III} centers. These complexes may also be synthesized by the chemical oxidation of $\text{Pt}(\text{pop})^4$ in the presence of halide ions. Mixed valence species of the type Pt_2X have also been observed transiently.

Excited-state studies demonstrated that $^3[\text{Pt}(\text{pop})^4]^*$ is a one-electron reductant in aqueous solution; it may also be quenched by halogen- or hydrogen-atom transfer by alkyl and aryl halides or by hydrogen-atom donors like alcohols, silanes, and stannanes. $\text{Pt}(\text{pop})^4$ is also known to catalytically produce hydrogen gas, as in the photochemical conversion of isopropyl alcohol to acetone and an equivalent of hydrogen. Furthermore, alkenes and alkynes both react with $^3[\text{Pt}(\text{pop})^4]^*$, either by energy transfer to effect photoisomerization or by hydrogen-atom abstraction to form an organic radical and Pt_2H .

1.4 Structural control of $^1\text{A}_{2u}$ -to- $^3\text{A}_{2u}$ intersystem crossing (ISC) in $\text{Pt}(\text{pop})$ by BF_2 functionalization

Due to its symmetric and relatively uncomplicated structure, $\text{Pt}(\text{pop})^4$ does not offer many opportunities for functionalization or derivatization. Replacement of the oxygen atoms in the P-O-P bridges by a methylene group curtails the reactive (and therefore greatly desired) $^3(d\sigma^*p\sigma)$ lifetime to only 55 ns.¹⁵ However, in 2011 Yan-Choi Lam and collaborators in the Bercaw group synthesized a derivative of $\text{Pt}(\text{pop})^4$ in which all eight hydrogen atoms of the pyrophosphito

groups are replaced with electron-withdrawing BF₂ groups, each of which links the oxygen atoms of two different bridges to form a cage-like structure (Figure 6).¹⁴

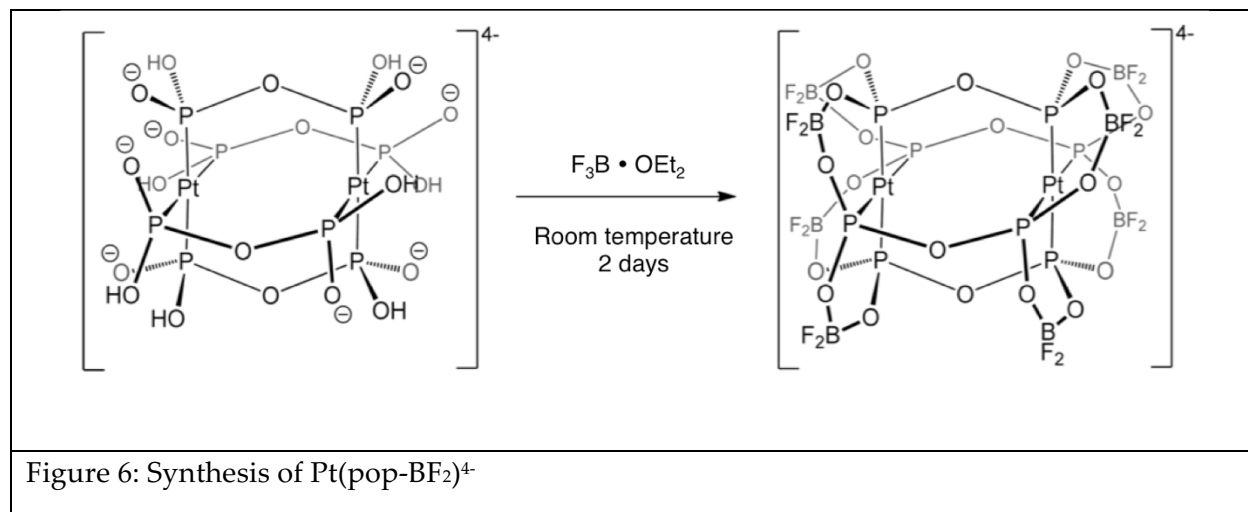


Figure 6: Synthesis of Pt(pop-BF₂)⁴⁻

This compound, per(difluoroboro)tetrakis(μ-pyrophosphito)diplatinate(II)⁴⁻, will be referred to as Pt(pop-BF₂)⁴⁻ for the remainder of this work. The electron-withdrawing nature of the BF₂ groups has the effect of removing electron density from the phosphorus atoms that are directly ligated to the Pt^{II} centers. This stabilizes the *dπ* levels in Pt(pop-BF₂)⁴⁻ compared to Pt(pop)⁴⁻, making it a stronger oxidant than the parent compound.

1.5 Photophysical implications of BF₂ functionalization

The “perfluoroboration” of Pt(pop) has dramatic effects on its photophysical properties. Table 1 compares the absorption and emission properties of Pt(pop)⁴⁻ and Pt(pop-BF₂)⁴⁻.¹⁴

Table 1: Comparison of Pt(pop) ⁴⁻ and Pt(pop-BF ₂) ⁴⁻		
Pt(pop-BF ₂) ⁴⁻	Pt(pop) ⁴⁻	Assignment

Absorption, nm (ϵ , M ⁻¹ cm ⁻¹)		
233 (7880)	246 (3770)	LMMCT
260 (3180)	285 (2550)	LMMCT
291 (2110)	315 (1640)	LMMCT
365 (37500)	372 (33400)	¹ (<i>dσ*→pσ</i>) ¹ A _{1g} → ¹ A _{2u}
454 (140)	454 (155)	³ (<i>dσ*→pσ</i>) ¹ A _{1g} → ³ A _{2u}
Emission, nm (Lifetime at 21 °C)		
393 (1.6 ns)	398 (~8 ps)	¹ (<i>pσ→dσ*</i>) ¹ A _{2u} → ¹ A _{1g}
512 (8.4 μs)	511 (9.4 μs)	³ (<i>pσ→dσ*</i>) ³ A _{2u} → ¹ A _{1g}
Emission Stokes Shift, cm ⁻¹		
1760	2230	Fluorescence
2460	2500	Phosphorescence
E _a for ISC (cm ⁻¹)		
2230	1190	¹ A _{2u} - ³ E _u S-O coupling

The metal-centered absorption features (the *dσ*→pσ* transitions) of Pt(pop-BF₂)⁴⁺ are similar to those of Pt(pop)⁴⁺; shifts of only about five hundred wavenumbers are observed. This is expected, as the BF₂ functionalization should not affect the *d→p* absorption features; the effect of the BF₂ groups is instead to stabilize the metal-centered orbitals as a whole. The most intense band at 365 nm (27397 cm⁻¹) results from the *dσ*→pσ* (¹A_{1g} → ¹A_{2u}) transition; the same transition in Pt(pop)⁴⁺ occurs at 372 nm (26881 cm⁻¹). The much more weakly absorbing spin forbidden singlet-to-triplet

($^1A_{1g} \rightarrow ^3A_{2u}$) transition occurs at 454 nm in Pt(pop-BF₂), the same as in the original compound (Figure 7 and Figure 4). All of the ligand-to-metal/metal charge transfer (LMMCT) absorption bands in Pt(pop-BF₂)⁴⁻ are blue-shifted by several thousand wavenumbers compared to Pt(pop)⁴⁻. This indicates that the ligand orbital energies are decreasing with respect to the metal orbitals. As the highest-energy occupied ligand orbitals are likely of oxygen origin, it stands to reason that an electron-withdrawing BF₂ group would decrease their energy and therefore raise the LMMCT transition energy. Although the BF₂ groups are also stabilizing the Pt centers, given the spectroscopically observed blue shift their effect on the ligand orbitals must be more dramatic.

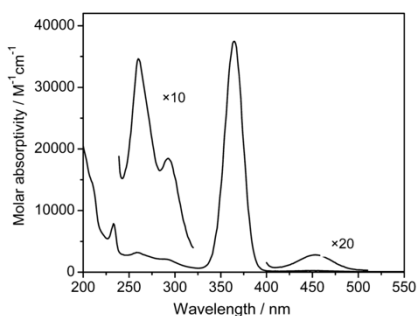


Figure 7: Absorption spectrum of Pt(pop-BF₂)⁴⁻.¹⁴

Compared to the absorbance spectra, the emission spectra of Pt(pop)⁴⁻ and Pt(pop-BF₂)⁴⁻ differ greatly. While both compounds exhibit very strong, long-lived phosphorescence at room temperature at ~512 nm, Pt(pop-BF₂)⁴⁻ has nearly equally strong fluorescence at 393 nm, while the corresponding fluorescence of Pt(pop)⁴⁻ at 398 nm is three orders of magnitude weaker as measured by emission quantum yields.¹⁴ Furthermore, the 1.6 ns fluorescence lifetime for Pt(pop-BF₂)⁴⁻ is over 500 times longer than the corresponding values of ~3 ps previously reported for Pt(pop)⁴⁻;¹⁶⁻¹⁸ this indicates that intersystem crossing (ISC) in Pt(pop-BF₂)⁴⁻ is much slower than in Pt(pop)⁴⁻.

Direct intersystem crossing (ISC) between states of identical symmetries (for example, $^1A_{2u} \rightarrow ^3A_{2u}$) is allowable only in point groups where one of the rotation components belongs to the totally symmetric representation; therefore, it is forbidden in the D_{4h} point group of Pt(pop)⁴⁻ and

Pt(pop-BF₂)⁴⁺. However, ISC may become partially allowed via spin-orbit coupling with higher triplet states. In Pt(pop)⁴⁺ and Pt(pop-BF₂)⁴⁺, this higher triplet state of interest is likely the ³E_u of LMMCT origin. By undergoing symmetry-allowed spin-orbit coupling with the ³E_u state, the ¹A_{2u} state is able to cross to the ³A_{2u} state, thus leading to the long-lived phosphorescence observed in both the Pt⁴⁺ complexes.

The 500-fold less rapid ISC in Pt(pop-BF₂)⁴⁺ versus Pt(pop)⁴⁺ is attributable to the fact that ISC results from spin-orbit coupling to an LMMCT state. The BF₂ groups lower the energy of the ligand states, as evidenced by the higher-energy LMMCT bands in the absorption spectra. A higher energy ³E_u state makes spin-orbit coupling with the ¹A_{2u} state less favorable, thereby slowing the rate of ISC in Pt(pop-BF₂)⁴⁺. Furthermore, solvent vibrations are quite important for acting as energy-accepting modes during ISC, as evidenced by the strong solvent dependence of Pt(pop)⁴⁺ decay kinetics.¹⁷ Given that BF₂ groups are both bulkier than the O-H···O- groups and that they form a rigid covalent cage rather than a more flexible hydrogen bonded one, one would expect that solvent interactions would be diminished. By that reasoning, the ability of the solvent to provide vibrational coupling between the singlet and triplet states is reduced for Pt(pop-BF₂)⁴⁺. The dramatic reduction in the rate of intersystem crossing and the concomitant increase in ISC activation energy, from 1190 cm⁻¹ for Pt(pop)⁴⁺ to 2230 cm⁻¹ for Pt(pop-BF₂)⁴⁺, is the reason for the much longer lived singlet in the perfluoroborated compound (1.6 ns vs 8 ps).

1.6 Electrochemical implications of BF₂ functionalization

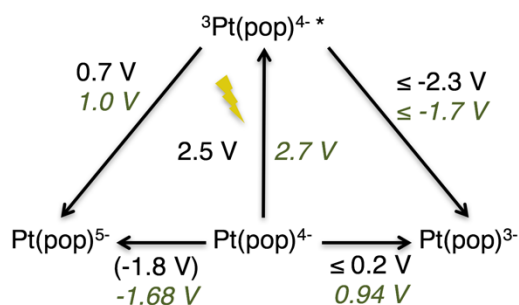


Figure 9: Latimer diagram for $\text{Pt}(\text{pop})^4$ and $\text{Pt}(\text{pop-BF}_2)^4$. Reduction potentials (all reported versus Fc^+/Fc)ⁱ for $\text{Pt}(\text{pop})$ are written in black;¹¹ reduction potentials for $\text{Pt}(\text{pop-BF}_2)$ are written in *green italics*.¹⁹

As discussed in section 1.4, the BF_2 groups were predicted to make $\text{Pt}(\text{pop-BF}_2)^4$ a stronger oxidant. Recent research published by myself and Bryan Hunter et al. places the potential of the reversible $\text{Pt}(\text{pop-BF}_2)^{4-/5-}$ couple at -1.68 V vs Fc^+/Fc while also predicting the existence of an even more reduced compound, $\text{Pt}(\text{pop-BF}_2)^{6-}$, due to a second irreversible reduction wave at -2.46 V.¹⁹ As expected, the single electron reduction potential for $\text{Pt}(\text{pop-BF}_2)^4$ lies at a more positive potential than that of $\text{Pt}(\text{pop})^4$. A Latimer diagram illustrating the electrochemical differences between the two compounds is presented in Figure 9. The excited state reduction potential for $^3[\text{Pt}(\text{pop-BF}_2)^4]^*$ is estimated based on spectroscopic data to be approximately 1.0 V, which makes it comparable in oxidative strength to compounds like $[\text{NO}]^+$ ($E^{\circ'} = 1.0$ V vs Fc/Fc^+ in CH_2Cl_2) and $[\text{Ru}(\text{phen})_3]^{3+}$ ($E^{\circ'} \approx 0.87$ V vs Fc/Fc^+ in CH_3CN).²⁰ Meanwhile, $^1[\text{Pt}(\text{pop-BF}_2)^4]^*$ is expected to have even *more* oxidizing power, as the spectroscopic difference between the absorption peaks for the triplet and the singlet is ≈ 5000 cm^{-1} , which corresponds to a 620 mV more positive potential. Given the short lifetime of the singlet state, it is improbable that this oxidizing power could be utilized in a diffusional solution setting; however, the possibilities for direct charge- or energy-transfer to substrates are substantial.

ⁱ Historic values for $\text{Pt}(\text{pop})^4$ were reported by Harvey in acetonitrile with respect to NHE; potentials were converted to a ferrocene reference by adding 0.64 V.

1.7 Applications

The oxidative strength of $[\text{Pt}(\text{pop-BF}_2)^4]^*$ and its steric bulk, combined with the fact that the production of the excited state is phototriggered, make it an attractive candidate for probing reactivity via transient absorption (TA) spectroscopy. As previously mentioned, canonical $\text{Pt}(\text{pop})^4$ is capable of performing a variety of organic transformations on its own due to the rotational flexibility of the terminal hydroxyl groups. This flexibility leaves the metal centers unblocked, and these open axial coordination sites on each Pt atom allow “docking” of various substrates with subsequent atom abstraction. The much more hindered and rigidly covalent BF_2 cage precludes this type of reactivity in $\text{Pt}(\text{pop-BF}_2)^4$. Unpublished results in the Gray Group obtained by Yan-Choi Lam indicate that $\text{Pt}(\text{pop-BF}_2)^4$ possesses very little, if any, of the inherent reactivity of $\text{Pt}(\text{pop})^4$ discussed in 1.3.3. For example, $\text{Pt}(\text{pop})^4$ reacts rapidly with iodomethane to form the oxidative addition product, but $\text{Pt}(\text{pop-BF}_2)^4$ is wholly unreactive toward such powerful electrophiles.²¹ However, considering the case where *only* electron transfer is desired from $\text{Pt}(\text{pop-BF}_2)^4$ to trigger reactivity in a *different* molecule, this lack of reactivity is actually quite a boon. Given its relative inertness, $\text{Pt}(\text{pop-BF}_2)^4$ is hoped to act as an outer sphere electron transfer agent only, with little or no inherent reactivity of its own. Meanwhile, the reduced (5-) and superreduced (6-) states are expected to be much more reactive than the parent compound and may act directly as catalytic agents. Initial studies in these areas will be discussed.

REFERENCES

- (1) Atoji, M.; Richardson, J. W.; Rundle, R. E. *J. Am. Chem. Soc.* **1957**, *79*, 3017.
- (2) Yam, V. W.-W.; Au, V. K.-M.; Leung, S. Y.-L. *Chem. Rev.* **2015**, *115*, 7589.
- (3) Mann, K. R.; Gordon, J. G.; Gray, H. B. *J. Am. Chem. Soc.* **1975**, *97*, 3553.
- (4) Smith, D. C.; Gray, H. B. *Coord. Chem. Rev.* **1990**, *100*, 169.
- (5) Fox, L. S.; Kozik, M.; Winkler, J. R.; Gray, H. B. *Science* **1990**, *247*, 1069.
- (6) Pan, Q.-J.; Fu, H.-G.; Yu, H.-T.; Zhang, H.-X. *Inorg. Chem.* **2006**, *45*, 8729.
- (7) Che, C. M.; Butler, L. G.; Gray, H. B. *J. Am. Chem. Soc.* **1981**, *103*, 7796.
- (8) Che, C. M.; Butler, L. G.; Gray, H. B.; Crooks, R. M.; Woodruff, W. H. *J. Am. Chem. Soc.* **1983**, *105*, 5492.
- (9) Bercaw, J. E.; Durrell, A. C.; Gray, H. B.; Green, J. C.; Hazari, N.; Labinger, J. A.; Winkler, J. R. *Inorg. Chem.* **2010**, *49*, 1801.
- (10) Stiegman, A. E.; Rice, S. F.; Gray, H. B.; Miskowski, V. M. *Inorg. Chem.* **1987**, *26*, 1112.
- (11) Harvey, E. L. Dissertation (Ph.D.), California Institute of Technology, 1990.
- (12) Heuer, W. B.; Totten, M. D.; Rodman, G. S.; Hebert, E. J.; Tracy, H. J.; Nagle, J. K. *J. Am. Chem. Soc.* **1984**, *106*, 1163.
- (13) Christensen, M.; Haldrup, K.; Bechgaard, K.; Feidenhans'l, R.; Kong, Q.; Cammarata, M.; Russo, M. L.; Wulff, M.; Harrit, N.; Nielsen, M. M. *J. Am. Chem. Soc.* **2008**, *131*, 502.
- (14) Durrell, A. C.; Keller, G. E.; Lam, Y.-C.; Sykora, J.; Vlček, A.; Gray, H. B. *J. Am. Chem. Soc.* **2012**, *134*, 14201.
- (15) King, C.; Auerbach, R. A.; Fronczek, F. R.; Roundhill, D. M. *J. Am. Chem. Soc.* **1986**, *108*, 5626.
- (16) van der Veen, R. M.; Cannizzo, A.; van Mourik, F.; Vlček, A.; Chergui, M. *J. Am. Chem. Soc.* **2010**, *133*, 305.
- (17) Milder, S. J.; Brunschwig, B. S. *J. Phys. Chem.* **1992**, *96*, 2189.
- (18) Vlček, A. 2016.
- (19) Darnton, T. V.; Hunter, B. M.; Hill, M. G.; Záliš, S.; Vlček, A.; Gray, H. B. *J. Am. Chem. Soc.* **2016**, *138*, 5699.
- (20) Connelly, N. G.; Geiger, W. E. *Chem. Rev.* **1996**, *96*, 877.
- (21) Lam, Y.-C.; Darnton, T. Unpublished results.